Supplement of Geosci. Model Dev., 19, 7069–7088, 2026
https://doi.org/10.5194/gmd-19-7069-2026-supplement
© Author(s) 2026. CC BY 4.0 License.

Geoscientific Model Development
Open Access
EGU

Supplement of

Sensitivity of Arctic mixed-phase cloud simulations to ice microphysical modifications in the WDM6 scheme of WRF (v4.3.1)

Hyun-Joon Sung et al.

Correspondence to: Baek-Min Kim (beakmin@pknu.ac.kr)

The copyright of individual parts of the supplement might differ from the article licence.

Contents of this file

Introduction

This supplement provides additional figures supporting the analysis presented in the main text. Figure S1 shows the three-dimensional flight track of the UND Citation aircraft during the M-PACE campaign, with the specific analysis segment highlighted.

Figure S2 presents the spatial distribution of low-level cloud fraction across all five model configurations, illustrating the systematic increase in cloud coverage from ice-dominated to liquid-dominated configurations.

Figure S3 decomposes the total IWC along the flight track into the cloud ice, snow, and graupel mixing ratios for all five configurations, showing that cloud ice dominates the ice budget in

WDM6 whereas snow becomes the dominant ice category in WDM6_ICE, and that nucleation modification (WDM6_IN) increases the snow contribution while leaving the total ice content close to that of WDM6.

Figure S4 presents the surface precipitation rate and accumulated snowfall at Utqiagvik (Barrow) for all five configurations, showing that the precipitation, which is almost entirely snowfall under the subzero conditions of this case, is largest in WDM6 and WDM6_IN and smallest in WDM6_ICE, consistent with the differences in cloud-ice-to-snow conversion among the experiments.

Figure S5 compares vertical profiles of temperature, potential temperature, relative humidity, and water vapor mixing ratio from radiosonde observations, ERA5 reanalysis, and the WDM6 and WDM6_ICE simulations, together with the diagnosed cloud-top heights, showing that the simulated inversion and cloud top are lower than observed and that this low bias is already present in the ERA5 boundary conditions and common to all configurations.

Figure S6 shows the vertical profiles of liquid and ice water content simulated with the Shin and Hong (2015) PBL scheme, confirming that the microphysical sensitivities identified in the main text are robust to the choice of boundary-layer parameterization.

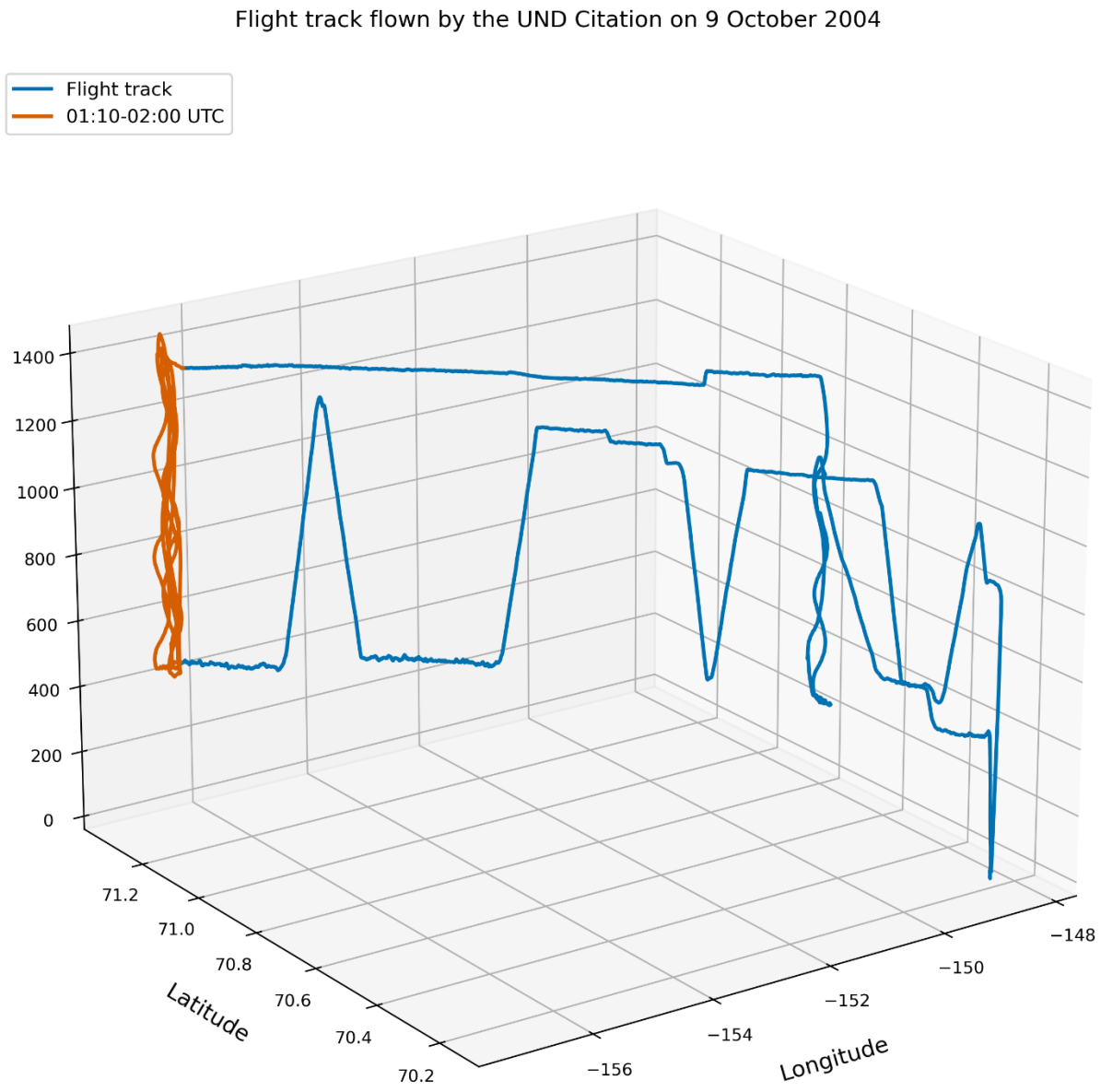

67

68 **Figure S1: 3D flight track of the UND Citation aircraft on 9 October 2004. The vermillion segment indicates the specific**
69 **analysis period (01:10–02:00 UTC).**

70

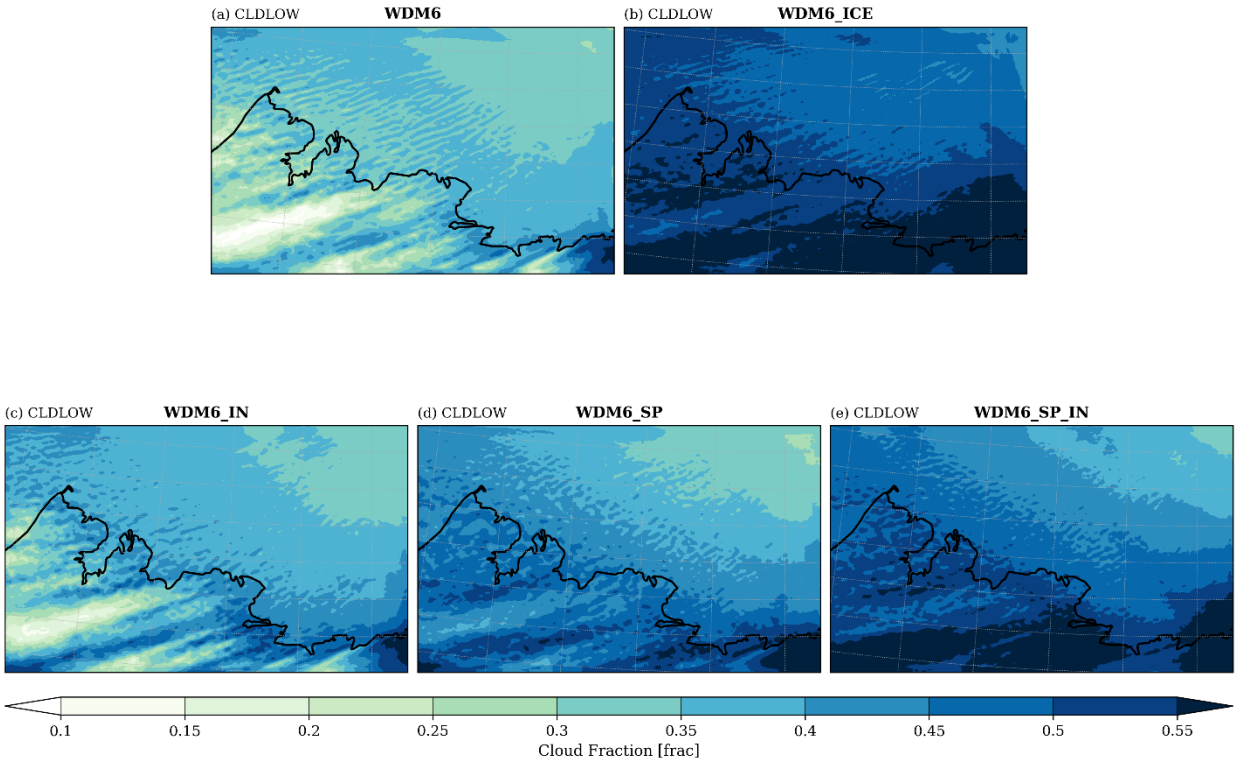

Figure S2: Time-averaged (12:00 UTC 9 October – 11:00 UTC 10 October 2004) low-level cloud fraction (CLDLOW; below 1500 m) from (a) WDM6, (b) WDM6_ICE, (c) WDM6_IN, (d) WDM6_SP, and (e) WDM6_SP_IN simulations over domain D03.

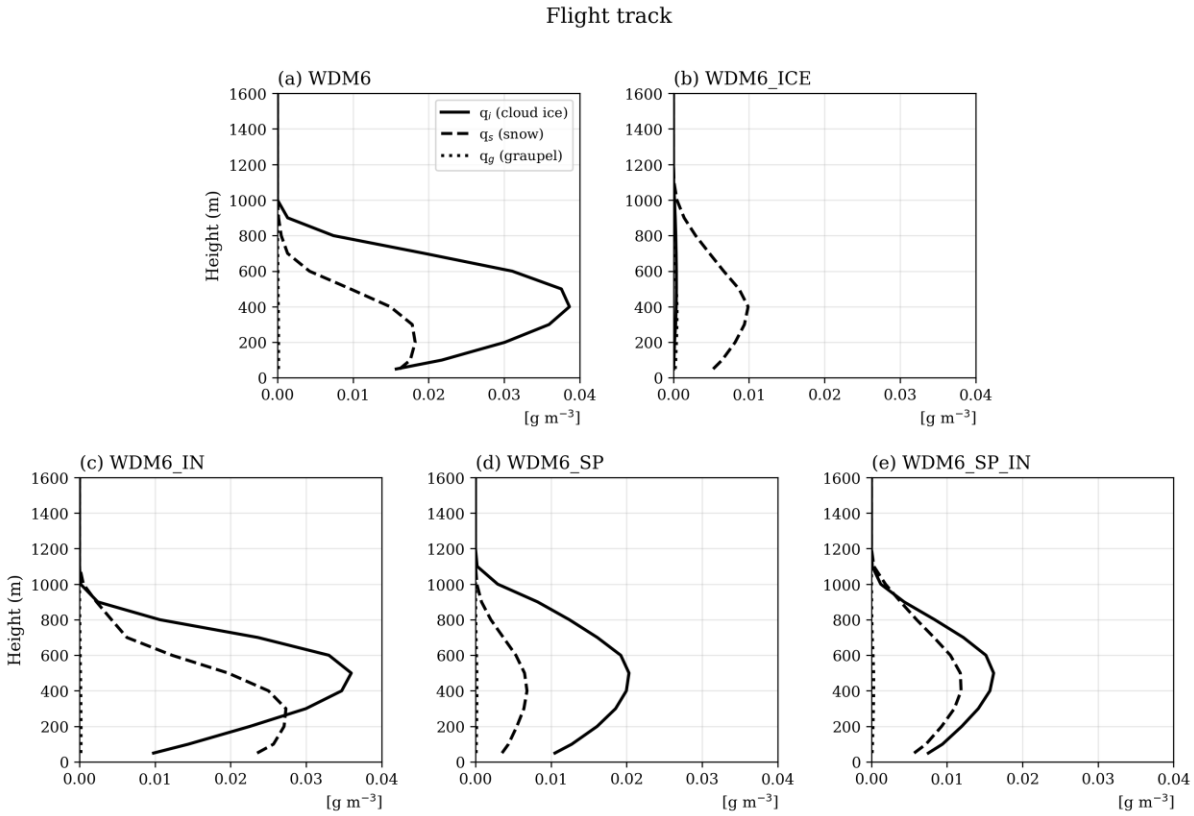

Figure S3: Decomposition of the total IWC along the flight track (Figure 3d) into cloud ice (q_i, solid), snow (q_s, dashed), and graupel (q_g, dotted) mixing ratios for (a) WDM6, (b) WDM6_ICE, (c) WDM6_IN, (d) WDM6_SP, and (e) WDM6_SP_IN, sampled between 01:00 and 02:00 UTC 10 October 2004.

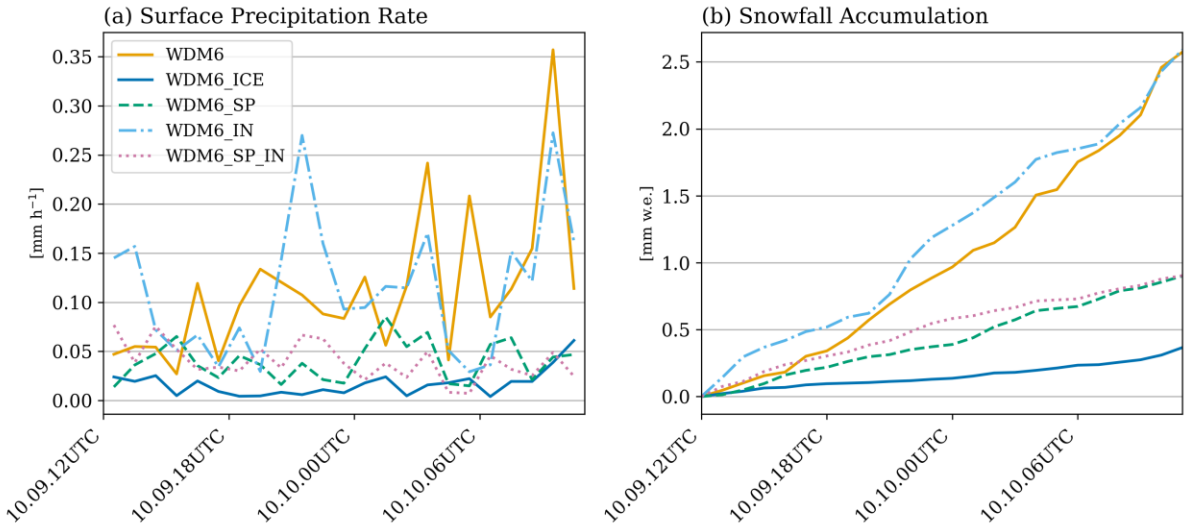

Figure S4: (a) Surface precipitation rate and (b) accumulated snowfall (water equivalent) at BAR over 12:00 UTC 9 October – 11:00 UTC 10 October 2004 for WDM6, WDM6_ICE, WDM6_SP, WDM6_IN, and WDM6_SP_IN.

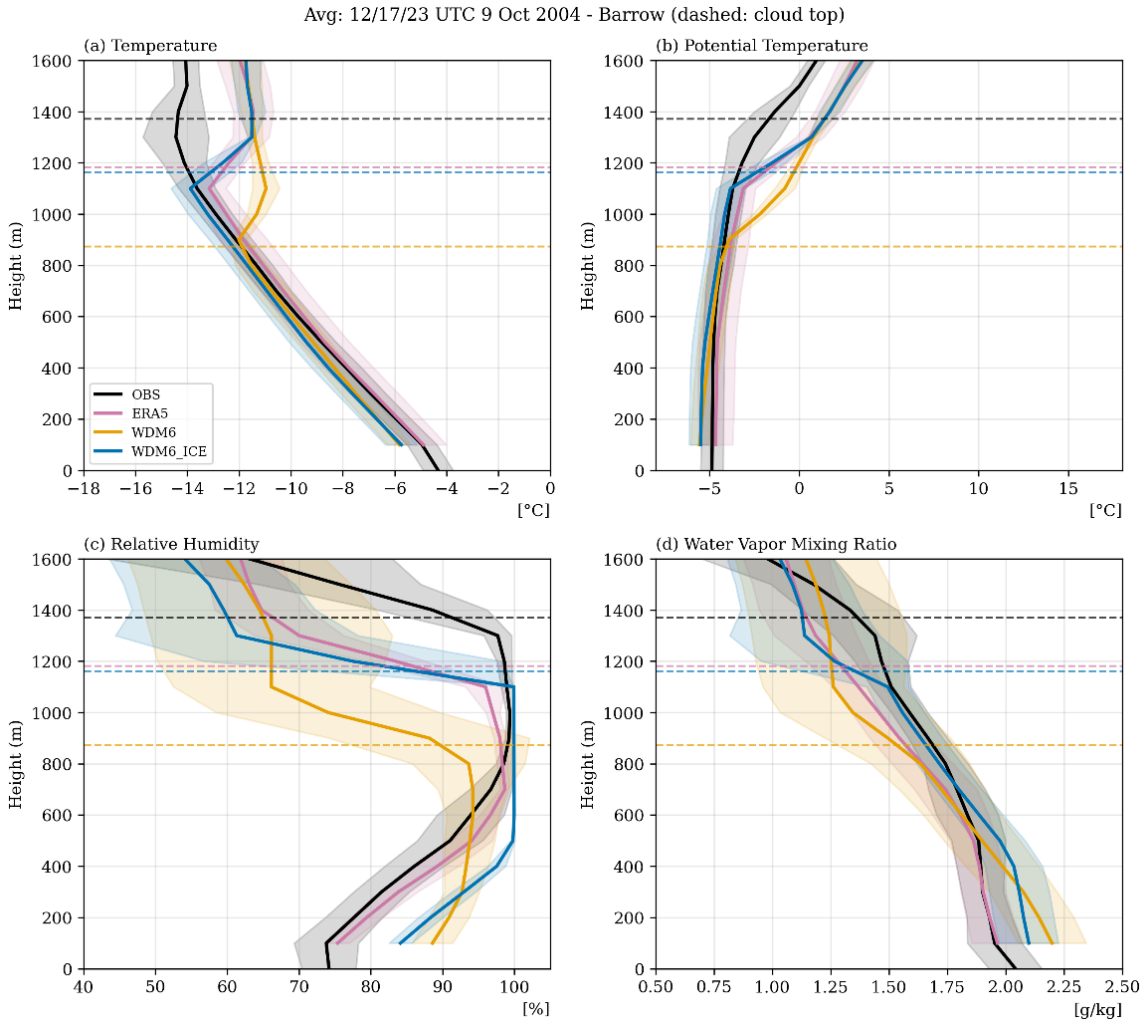

Figure S5: Vertical profiles of (a) temperature, (b) potential temperature, (c) relative humidity, and (d) water vapor mixing ratio at Utqiagvik (Barrow), averaged over three radiosonde times (12, 17, 23 UTC 9 October 2004), for the observations (radiosonde), ERA5, WDM6, and WDM6_ICE. Dashed horizontal lines indicate the diagnosed cloud-top height for each source. Because condensate mixing ratios are not available from the radiosondes, the observed cloud top is defined as the highest level with relative humidity exceeding 95%, whereas for ERA5 and the simulations it is defined as the highest level with total condensate mixing ratio exceeding 10^{-6} kg kg^{-1}, which is the more appropriate criterion for the model fields.

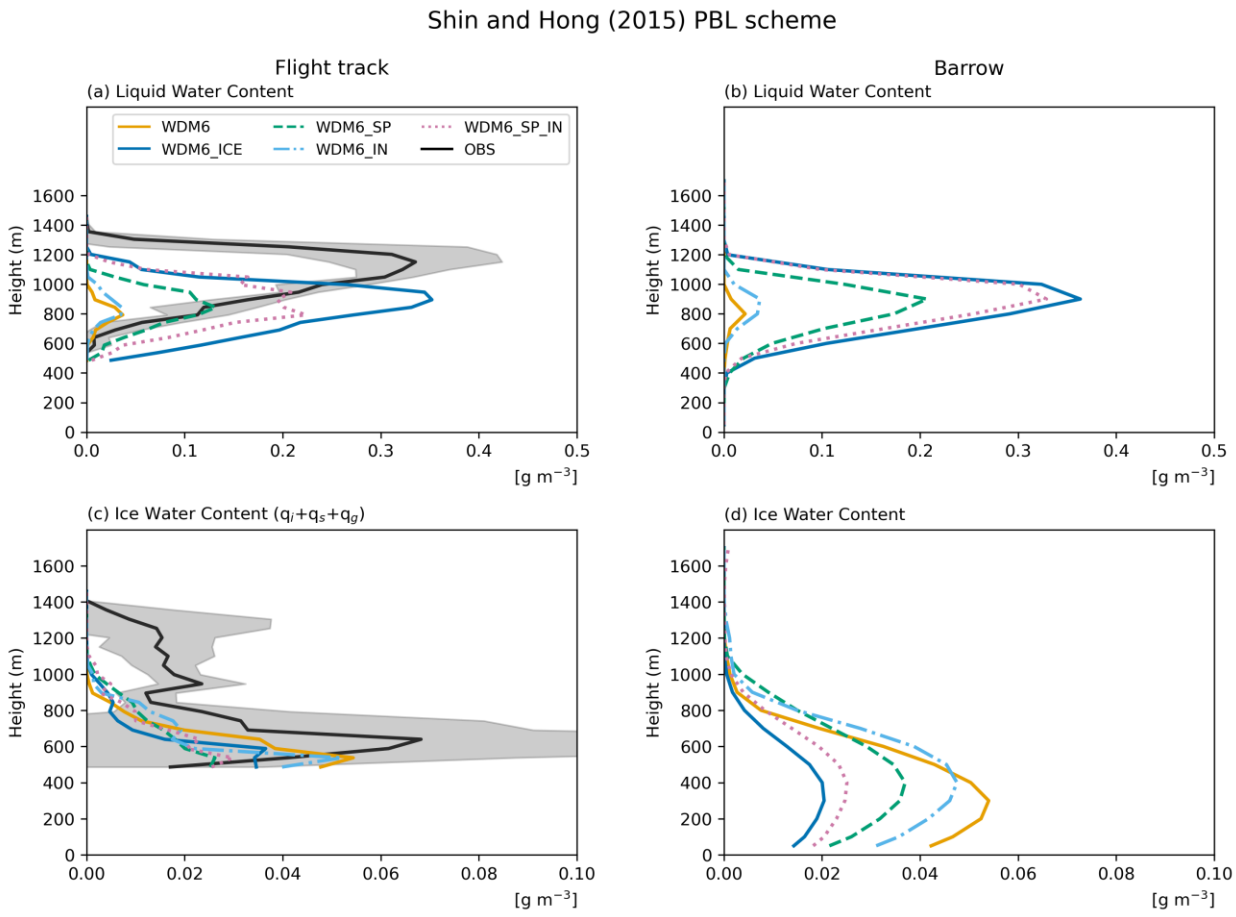

Figure S6. Vertical profiles of (a, b) LWC and (c, d) IWC simulated with the Shin and Hong (2015) PBL scheme. The left column (a, c) shows the profile sampled along the flight track during 01:00 – 02:00 UTC 10 October 2004, and the right column (b, d) shows the time-averaged (12:00 UTC 9 October – 11:00 UTC 10 October 2004) profile at BAR. Black solid lines with gray shading indicate observations (±1σ), and colored lines represent sensitivity experiments: WDM6 (orange, solid), WDM6_ICE (blue, solid), WDM6_SP (green, dashed), WDM6_IN (sky blue, dash-dot), and WDM6_SP_IN (purple, dotted).